Am J Transl Res 2019;11(1):257-268
www.ajtr.org /ISSN:1943-8141/AJTR0084841

Original Article

Vascular endothelial Cdc42 deficiency delays skin wound-healing processes by increasing IL-1β and TNF-α expression

Mengying Xu[1], Jiawen Lv[3], Ping Wang[2], Yanxia Liao[1], Yiran Li[1], Wen Zhao[4], Junchao Zen[1], Zheyu Dong[5], Zihao Guo[5], Xiaoyin Bo[5], Min Liu[5], Lin Zhang[2], Guodong Hu[1], Yinghua Chen[2]

[1]Department of Respiratory and Critical Care Medicine, Nanfang Hospital, Southern Medical University, Guangzhou 510515, China; [2]Guangdong Provincial Key Laboratory of Construction and Detection in Tissue Engineering, Department of Histology and Embryology, School of Basic Medical Sciences, Southern Medical University, Guangzhou 510515, China; [3]Department of Respiratory and Critical Care Medicine, Nanjing General Hospital of Nanjing Military Region, Nanjing, China; [4]Department of Medical Imaging, The Third Affiliated Hospital of Southern Medical University, Guangzhou 510515, China; [5]Southern Medical University, Guangzhou 510515, China

Received May 8, 2018; Accepted December 18, 2018; Epub January 15, 2019; Published January 30, 2019

Abstract: Angiogenesis is an important step in skin wound repair. Angiogenesis is affected by the functions of many types of cells, especially endothelial cells. Cdc42 plays a vital role in endothelial cell function and vascular development; however, the role of Cdc42 in skin microvascular permeability and skin wound healing is unclear. This study investigated the involvement of Cdc42 in skin wound-healing processes based on its known roles in angiogenesis. Full-thickness skin wounds were created on wild-type and inducible vascular-endothelial-specific *Cdc42*$^{-/-}$ mice. *Cdc42* deletion in endothelium affected wound healing in following ways. Reepithelialization of wounds in *Cdc42*$^{-/-}$ mice was delayed compared with that of wounds in wild-type mice. The degree of angiogenesis of wound granulation tissue was significantly lower in *Cdc42*$^{-/-}$ mice than in wild-type mice. Infiltration of F4/80+ macrophages and the expression of MCP-1, IL-1β, and TNF-α were increased in the wound bed of *Cdc42*$^{-/-}$ mice compared with wild-type mice. These results confirm that Cdc42 in endothelium is required for angiogenesis and is an essential regulator of key skin wound-healing processes.

Keywords: Cdc42, skin wound, angiogenesis, reepithelialization, inflammation

Introduction

Skin is the most important barrier against harmful environmental factors, and as a result, efficient and complete skin wound repair is critical. Skin wound healing is a complex process involving various cells and chemokines. This process occurs via three distinct yet overlapping phases: inflammation, proliferation, and remodeling [1, 2]. The proliferation phase includes reepithelialization, endothelial proliferation, angiogenesis, and granulation tissue formation. Then, keratinocytes polarize and migrate, ultimately leading to the stratification and differentiation needed to reconstruct the skin barrier. In the remodeling phase, granulation tissue is replaced by collagenous scar tissue.

Angiogenesis, the formation of new blood vessels from existing ones, plays an important role in wound repair. The functions of various cell types, especially endothelial cells, contribute to angiogenesis [3]. In healing wounds, the number of new blood vessels are approximately 2-3 times greater and as high as 10 times greater than that in normal tissue [4], These blood vessels speed up wound healing by transporting nutrients and oxygen to the wound site. Impaired angiogenesis or endothelial precursor cell dysfunction can retard wound healing [5, 6]. For example, diabetic mice do not generate a sufficient number of new blood vessels, leading to poor healing [7, 8]. In the clinic, non-healing wounds are a substantial health problem for individuals with accidental, surgical, or chronic skin lesions [9, 10]. Many previous and ongoing

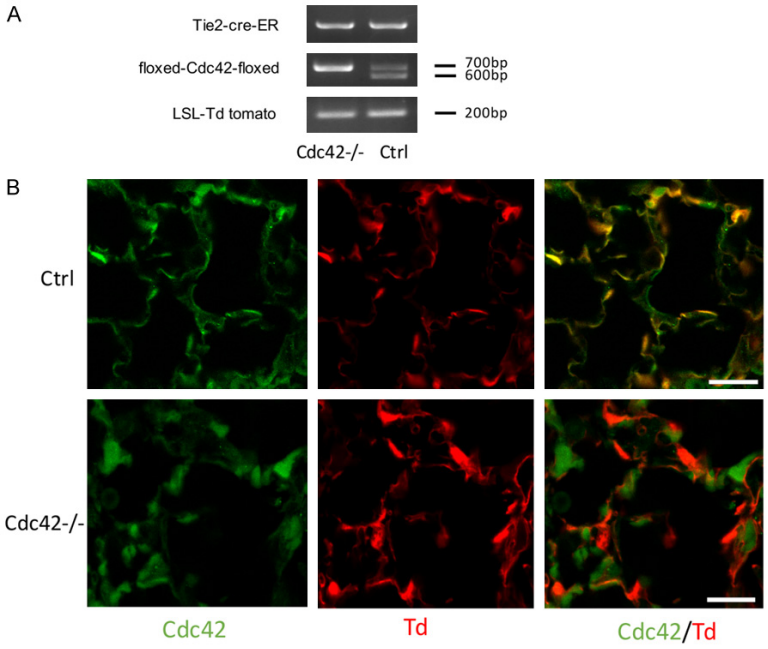

Figure 1. Generation of vascular endothelial-cell-specific *Cdc42*$^{-/-}$ mice. A. PCR genotyping was performed using genomic DNA collected from tails of control (Ctrl) and *Cdc42*$^{-/-}$ mice. The upper panel shows PCR products for the Tie2-Cre-ER allele (900 bp), the middle panel shows those for the Cdc42$^{L/L}$ allele (700 bp for *Cdc42*$^{-/-}$ and 600 and 700 bp for Ctrl mice), the bottom panel shows those of the Lox-Stop-Lox tdTomato allele (200 bp). B. Representative images of tdTomato fluorescence (red) in lung samples of Ctrl and *Cdc42*$^{-/-}$ mice counterstained with a fluorescent anti-Cdc42 antibody (green). Cdc42 was absent from the endothelium and present in alveolar epithelium in *Cdc42*$^{-/-}$ mice. White scale bars = 25 μm.

studies have investigated the factors involved in the function of blood vessel endothelial cells as it relates to wound healing.

Cdc42 is a Rho family small GTPase that is ubiquitously expressed [11]. Rho GTPases, including RhoA, Rac1, and Cdc42, are important molecules that affect microvascular permeability. RhoA enhances permeability, whereas Rac1 and Cdc42 strengthen barrier function [12, 13]. Cdc42 was reported to play a vital role in endothelial cell function and vascular development [14]. With respect to endothelial permeability, Cdc42 alters endothelial cell junctions and boosts intercellular barrier function by inducing an interaction between a-catenin and the VE-cadherin complex [15]. However, the role of Cdc42 in skin microvascular permeability and skin wound healing is unclear. Our previous experiments confirmed that global knockout of Cdc42 in endothelia was embryonic lethal [16]. Therefore, we constructed the Cre-recombination-based mouse model with an inducible vascular-endothelial-specific *Cdc42* deletion. Here, we investigate the hypothesis that Cdc42 is a crucial regulator of skin wound-healing processes.

Materials and methods

Animals

Conditional *Cdc42*$^{-/-}$ mice and Lox-Stop-Lox tdTomato mice were a gift from Professor Yi Zheng from the University of Cincinnati, USA. Tie2-cre-ER mice were obtained from the Gaiger laboratory in Germany. In these mice, the CRE recombinant enzyme is expressed only in vascular endothelial cells after induction with tamoxifen. Mice were housed 4-5 per cage in controlled conditions (temperature: 24 ± 1°C and lighting: 12 hr light/dark cycle) with food and water ad libitum. All animal experiments were performed in accordance with the regulations of the University of Southern Medical Animal Care Committee. Using the Cre/Loxp knockout technique, we crossed the conditional *Cdc42*$^{-/-}$ with Tie2-Cre-ER mice. The resulting mice were crossed with Lox-Stop-Lox tdTomato mice to generate the vascular-endothelial-specific target mice (hereafter referred to as *Cdc42*$^{-/-}$ mice).

Animal treatments

When the mice were 4 weeks old, they were injected intraperitoneally (i.p.) with tamoxifen (1 mg/d; Cayman Chemical, USA) for 4 days to induce the *Cdc42* knockout. Two weeks later, mice were anesthetized with an i.p. injection of pentobarbital. A 6 × 6-mm-square full-thickness skin wound was created on the left or right dorsal skin. The wounds were allowed to dry to form a scab. The wounds were photographed and measured every 2 days, using a measuring tape to standardize the image dimensions. Whole wound sites, including the scab and epithelial margins, were collected on

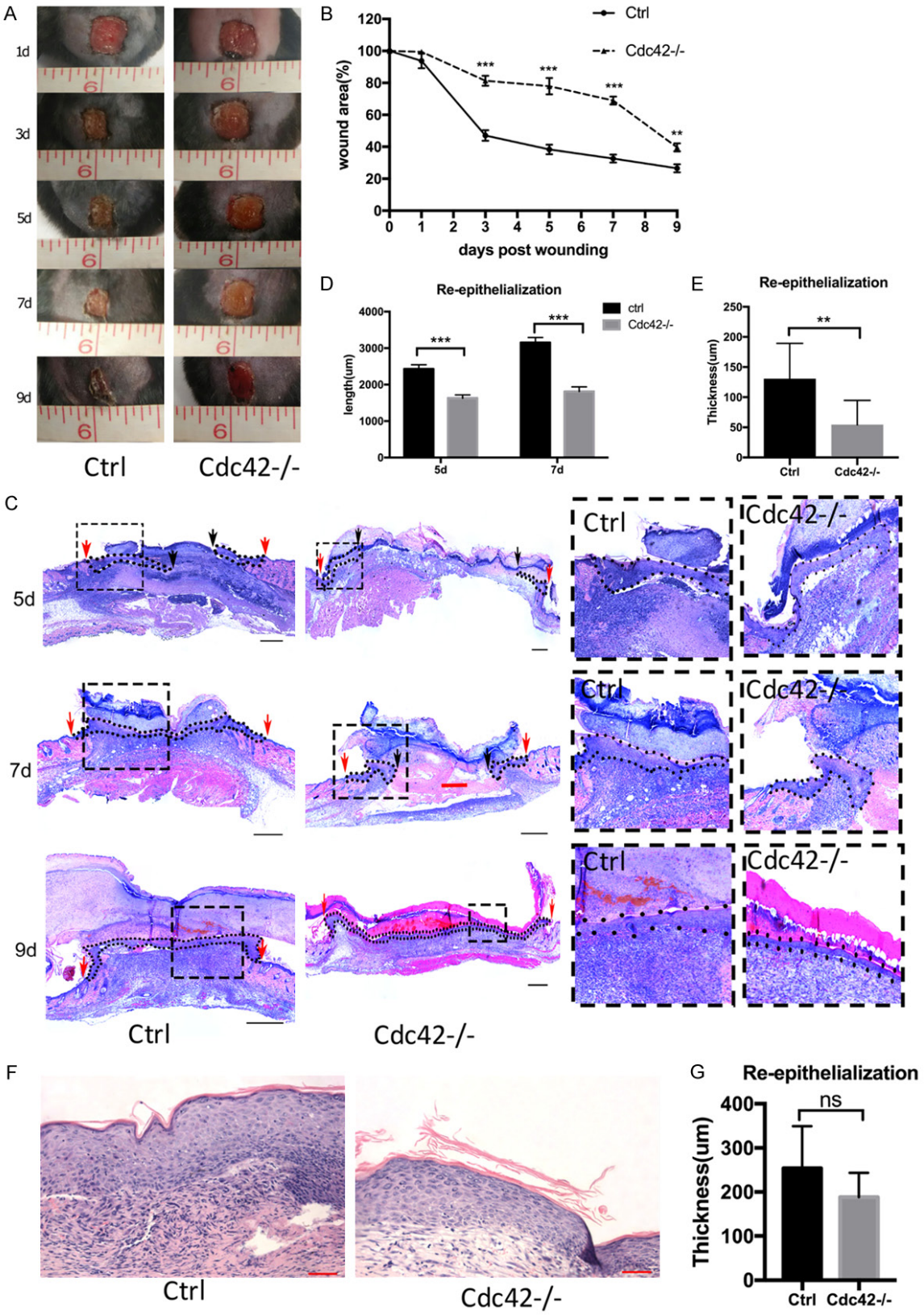

Figure 2. Delayed wound healing in *Cdc42*$^{-/-}$ mice. A. Representative images of healing wounds in *Cdc42*$^{-/-}$ and Ctrl mice. B. Quantification of open wound area showed wound closure occurred significantly more slowly in wounds of *Cdc42*$^{-/-}$ mice compared with Ctrl mice (n = 3). C. Representative images of histological sections of wounds in Ctrl and *Cdc42*$^{-/-}$ mice at days 5, 7, and 9 post-wounding. High-magnification images of the wounded areas denoted

by black dashed squares are shown to the right. Sections were stained with HE. D. Quantification of the lengths of epithelial tongues at days 5 and 7 post-wounding indicated that reepithelialization occurred significantly more slowly in *Cdc42*$^{-/-}$ mice compared with Ctrl mice (n = 3). E. The average thickness of wounds at day 9 post-wounding was significantly decreased in *Cdc42*$^{-/-}$ skin compared with Ctrl skin (n = 5). F. Representative images of histological sections of the wounds in control and *Cdc42*$^{-/-}$ mice at day 14 post-wounding. G. The average thickness of wounds at day 14 post-wounding was not different between *Cdc42*$^{-/-}$ skin compared with Ctrl skin (n = 5). Black scale bars = 500 μm; red scale bars = 100 μm; *P* values: **< .05; ***< 0.01; ns, not significant.

days 3, 5, 7, 9, and 14. The skin samples were divided, with one half fixed with 4% paraformaldehyde (Sigma-Aldrich, USA) for histological analysis and the other half frozen in liquid nitrogen for enzyme-linked immunosorbent assay (ELISA) analysis.

Wound-closure rate measurements

At each timepoint, the wound area was analyzed using ImageJ (Software 1.51m9, Wayne Rasband, National Institutes of Health, USA). The wound-area percentage was calculated as follows: wound area (%) = [($area_{day\ n}$)/$area_{day\ 0}$] × 100 [17].

Bromodeoxyuridine (BrdU) labeling

Prior to collecting the wound sites, mice were treated with a BrdU solution (20 mg/ml, 0.1 ml i.p. injection) and transferred to the dark for 2 h prior to sacrifice. Histological sections from the middle of the wound were washed with 3% hydrogen peroxide for 15 min, 2 M HCl for 30 min, and boric acid for 15 min before being incubated with anti-BrdU antibody (1:50, sc-32323, Santa Cruz) overnight at 4°C and then incubated with a secondary antibody.

Histology and immunohistochemistry

After wounded skin tissues were collected, they were fixed in 4% paraformaldehyde and embedded in paraffin. Sections 4-μm thick were cut from paraffin blocks, transferred to glass slides, and used for hematoxylin & eosin (HE), Masson's trichrome, toluidine blue, and immunohistochemical staining. Morphological alterations in the skin were inspected using light microscopy. Epithelial tongue length was measured as the distance from the tip of epithelial tongue to the unwounded dermis. The average epithelial tongue thickness was approximated using the equation: (area of epithelial tongue)/(length of epithelial tongue). For immunostaining, sections were deparaffinized and rehydrated and blocked with 10% goat serum at room temperature for 60 min. Then, sections were incubated overnight at 4°C with anti-keratin 1 (K1) antibody (1:100, catalog #905204, BioLegend), anti-keratin 6 (K6) antibody (1:100, catalog #905701, BioLegend), anti-CD31 antibody (catalog #00084985, Dako), anti-F4/80 antibody (1:100, catalog #144-80182, eBioscience), or anti-α-smooth muscle actin (SMA) antibody (catalog #BM0002, Boster Biological Technology) and incubated with a species-specific secondary antibody for 1 hour. Then, stained sections were examined and imaged using a microscope (Leica-CTR-4000). The microscopic field centered on the wound site in the immunostained sections, and the numbers of F4/80-positive macrophages and CD31-positive blood vessels were counted.

ELISA

The previously frozen tissue was homogenized in extraction solution (100 mg tissue in 1 ml 0.1 nM phosphate-buffered saline) using OMNI Ruptor 4000. The suspension was spun at 5000 × g for 10 min at 4°C, and the supernatant was used for ELISA. ELISAs were performed using kits for murine interleukin 1β (IL-1β, E-EL-M0037c, Elabscience, Houston, TX, USA) and tumor necrosis factor α (TNF-α, E-EL-M0049c, Elabscience) according to the manufacturer's instructions.

Statistical analysis

All numeric data are presented as mean ± standard error of the mean and were analyzed using SPSS v19.0 software. The statistical significance of the differences between experimental groups was determined using the Student's *t*-test. *P* values < 0.05 were considered significant.

Results

Generation of inducible vascular-endothelial-cell-specific Cdc42-deficient mice

Mice were bred as described and offspring were genotyped to verify the presence of the Tie2-Cre-ER, floxed Cdc42, and Lox-Stop-Lox tdTomato alleles. Mice with the targeted geno-

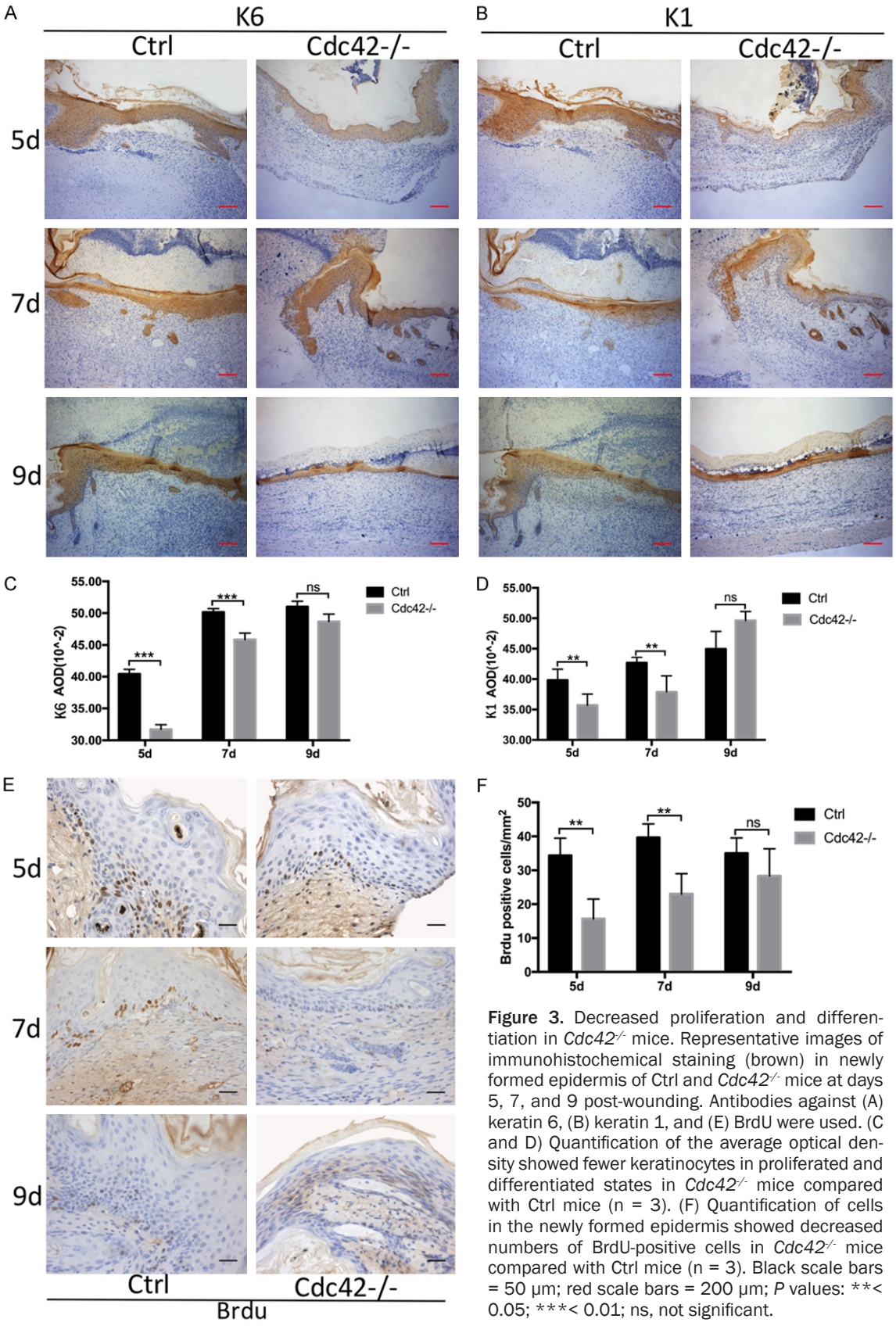

Figure 3. Decreased proliferation and differentiation in *Cdc42*$^{-/-}$ mice. Representative images of immunohistochemical staining (brown) in newly formed epidermis of Ctrl and *Cdc42*$^{-/-}$ mice at days 5, 7, and 9 post-wounding. Antibodies against (A) keratin 6, (B) keratin 1, and (E) BrdU were used. (C and D) Quantification of the average optical density showed fewer keratinocytes in proliferated and differentiated states in *Cdc42*$^{-/-}$ mice compared with Ctrl mice (n = 3). (F) Quantification of cells in the newly formed epidermis showed decreased numbers of BrdU-positive cells in *Cdc42*$^{-/-}$ mice compared with Ctrl mice (n = 3). Black scale bars = 50 μm; red scale bars = 200 μm; *P* values: **< 0.05; ***< 0.01; ns, not significant.

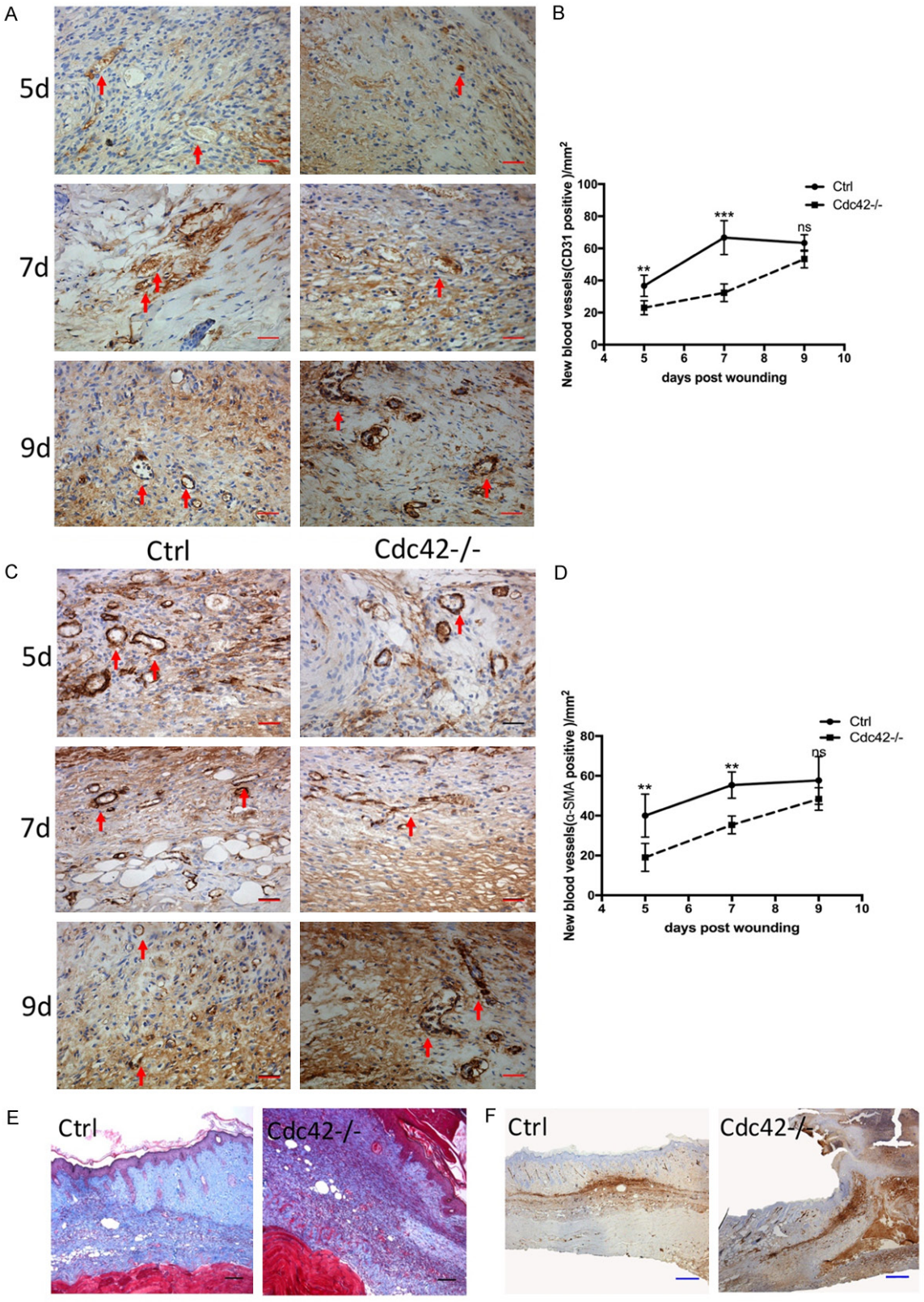

Figure 4. Decreased collagen fiber formation and angiogenesis in *Cdc42*$^{-/-}$ mice. A. Representative images of CD31 immunohistochemical staining (brown) in wounds of Ctrl and *Cdc42*$^{-/-}$ mice at day 7 post-wounding. B. Quantification of CD31-positive cells per mm^2 showed less angiogenesis in *Cdc42*$^{-/-}$ mice compared with Ctrl mice (n = 3). C. Representative images of α-SMA immunohistochemical staining (brown) in granulation tissue of Ctrl and *Cdc42*$^{-/-}$

mice at days 5, 7, and 9 post-wounding to show angiogenesis. D. Quantification of α-SMA-positive cells per mm^2 showed less angiogenesis in *Cdc42*$^{-/-}$ mice compared with Ctrl mice (n = 3). E. Representative images of Masson's staining of the wound site at day 7 post-wounding. Blue: collagen fibers and mucus, red: muscle and elastic fibers, blue-brown: nucleus. F. α-SMA was detected to show myofibroblasts. Black scale bars = 200 μm; red scale bars = 50 μm; blue scale bars = 500 μm; *P* values: **< 0.05, ***< 0.01; ns, not significant.

type were selected for the *Cdc42*$^{-/-}$ mice group, and their littermates were used as controls (Ctrl mice, **Figure 1A**). Because normal skin lacks extensive vascular tissue, we evaluated lung tissue to determine if mice were Cdc42-deficient. The vascular endothelial cells of mice with tdTomato alleles fluoresce red when the target gene is knocked out, so we looked for colocalization of Cdc42 expression and tdTomato fluorescence. The lung tissue of target mice showed no colocalization of Cdc42 and tdTomato fluorescence (**Figure 1B**).

The effect of Cdc42 knockout on the wound-healing process

First, we compared the skin structure of *Cdc42*$^{-/-}$ mice with Ctrl mice. There were no differences in skin structure between the two groups prior to creating the wound (Supplementary Figure 1). Next, skin wounds were created in both groups. Visual assessment showed that the healing rate of *Cdc42*$^{-/-}$ mice was lower than that in Ctrl mice (**Figure 2A** and **2B**). HE staining showed that wounds in Ctrl mice were almost completely healed, with reepithelialization apparent by day 7, whereas those in *Cdc42*$^{-/-}$ mice were not completely healed until day 9. The rate of wound reepithelialization was significantly slower in *Cdc42*$^{-/-}$ mice than in Ctrl mice (**Figure 2C-E**). By day 14, the epithelial thickness was not different between the two groups (**Figure 2F** and **2G**).

The effect of Cdc42 knockout on the proliferation and differentiation of keratinocytes

We next investigated the proliferation and differentiation of keratinocytes. The expression of K6 is closely associated with cell proliferation, and K1 is often used as a marker of normal keratinocytes differentiation [18, 19]. At days 5 and 7 post-wounding (i.e., the reepithelialization stage), the wounds of *Cdc42*$^{-/-}$ mice had fewer keratinocytes in proliferating and differentiating states than those of Ctrl mice (**Figure 3A-D**). In addition, the number of BrdU-positive cells in regenerated epidermis was significantly higher in Ctrl mice than in *Cdc42*$^{-/-}$ mice on days 5 and 7 post-wounding (**Figure 3E** and **3F**). These results indicated that *Cdc42*$^{-/-}$ mice have a decreased rate of re-epithelialization likely due to altered rates of keratinocyte proliferation.

The effect of Cdc42 knockout on angiogenesis and collagen remodeling

To evaluate the effect of Cdc42 knockout on angiogenesis, we used wound angiogenesis density as an angiogenic indicator. Angiogenesis was evaluated based on the number of CD31-positive cells (**Figure 4A** and **4B**) and α-SMA-positive cells (**Figure 4C** and **4D**) in granulation tissue. Neovascularization was significantly decreased in *Cdc42*$^{-/-}$ mice compared with Ctrl mice.

To evaluate the effect of Cdc42 knockout on collagen remodeling, we investigated the levels of Masson's staining and α-SMA expression. There were significantly fewer collagen fibers in granulation tissue of *Cdc42*$^{-/-}$ mice than in Ctrl mice based on Masson's staining (**Figure 4E**). Similarly, the expression of α-SMA was lower in *Cdc42*$^{-/-}$ mice than in Ctrl mice, indicating fewer numbers of myofibroblasts [20] (**Figure 4F**).

Cdc42 knockout increased macrophage aggregation but did not affect other inflammatory cells

Because Cdc42 is an important regulator of endothelial permeability [15], we examined the effect of Cdc42 deletion on immune-cell populations within wounded skin on days 5 and 7 post-wounding. Typically, macrophages infiltrate the wound and become part of the granulation tissue [21]. Based on F4/80 staining, the number of macrophages in the granulation tissue of *Cdc42*$^{-/-}$ mice was greater than that of Ctrl mice (**Figure 5A** and **5B**). T lymphocytes and mast cells were also detected in the wound bed and adjacent tissue, but no significant differences were observed between the wound tissue of Ctrl and *Cdc42*$^{-/-}$ mice at days 5 and 7 post-wounding (**Figure 5C-F**). These results indicate that Cdc42 deletion increased macrophage aggregation in the wound.

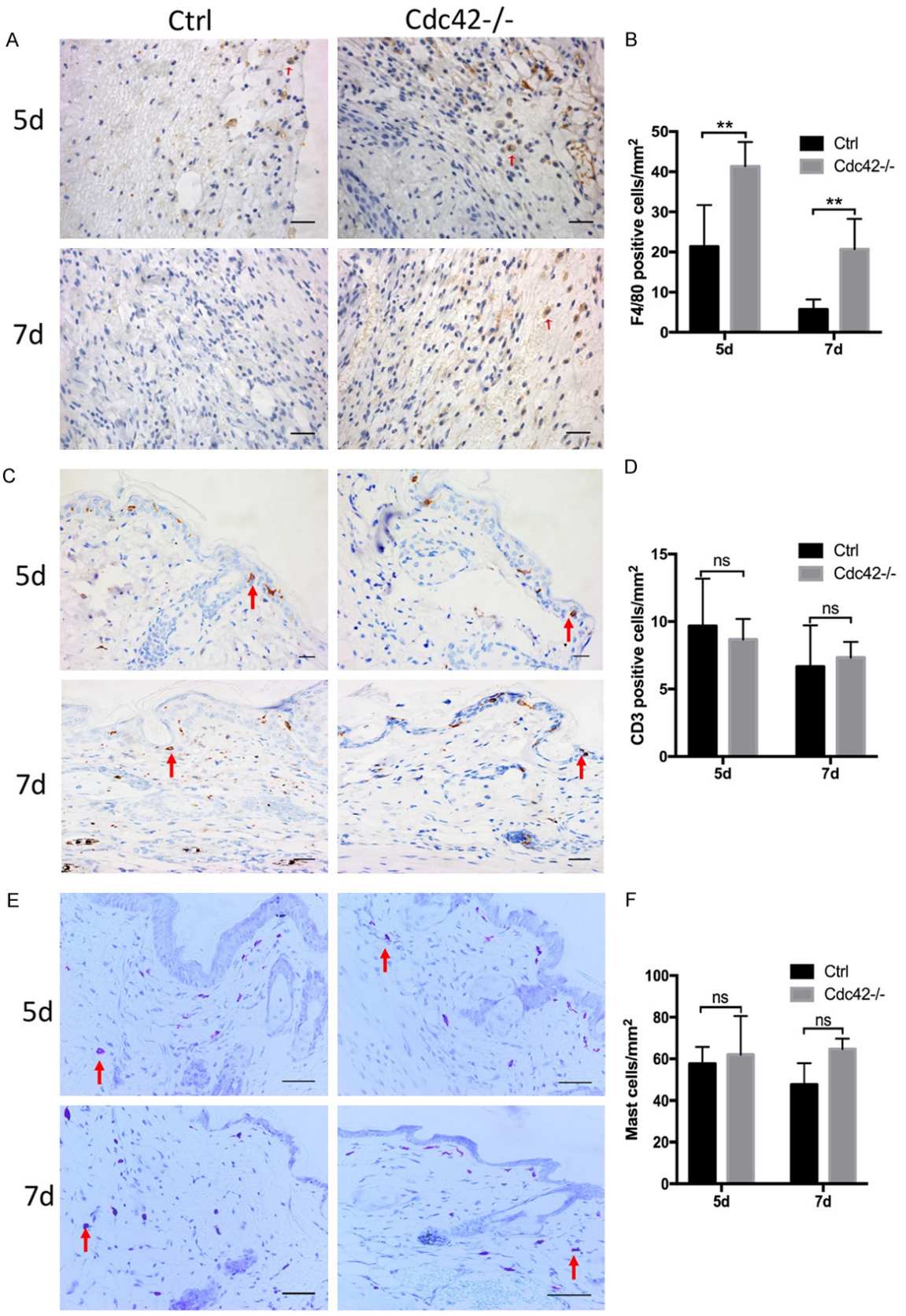
Ctrl
Cdc42-/-
A
5d
7d
B
F4/80 positive cells/mm²
Ctrl
Cdc42-/-
**
**
5d
7d
C
5d
7d
D
CD3 positive cells/mm²
Ctrl
Cdc42-/-
ns
ns
5d
7d
E
5d
7d
F
Mast cells/mm²
Ctrl
Cdc42-/-
ns
ns
5d
7d

Figure 5. Increased immune infiltration in *Cdc42*$^{-/-}$ mice. A. Representative images of F4/80 immunohistochemical staining (brown) to detect macrophages at days 5 and 7 post-wounding. B. Quantification of F4/80-positive cells per mm^2 increased macrophage infiltration in *Cdc42*$^{-/-}$ mice compared with Ctrl mice (n = 3). C. Representative images of CD3 immunohistochemical staining (brown) to detect T cells at days 5 and 7 post-wounding. D. Quantification of CD3-positive cells per mm^2 showed no significant differences between the two groups (n = 3). E. Representative images of toluidine blue staining (dark purple) to detected mast cells at days 5 and 7 post-wounding. F. Quantification of mast cells per mm^2 showed no significant differences between the two groups (n = 3). Black scale bars = 50 μm; *P* values: **< 0.05; ns, not significant.

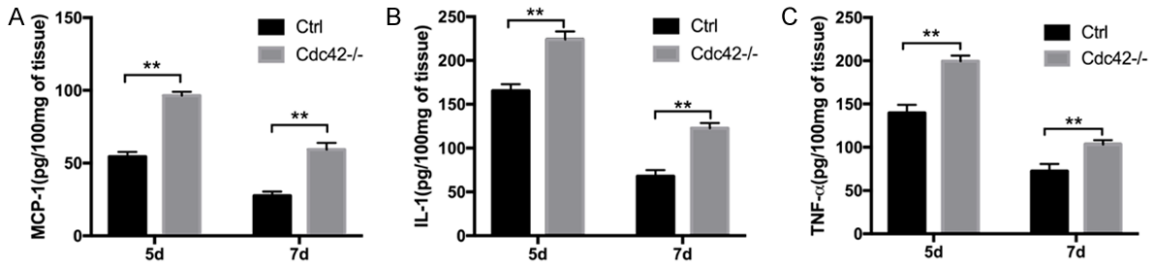

Figure 6. Increased cytokine levels in *Cdc42*$^{-/-}$ mice. Levels of (A) MCP-1, (B) IL-1β, and (C) TNF-α were increased in wounds of *Cdc42*$^{-/-}$ mice compared with Ctrl mice. MCP-1, IL-1β, and TNF-α were detected using ELISA at days 5 (n = 3) and 7 (n = 3) post-wounding. *P* values: **< 0.05.

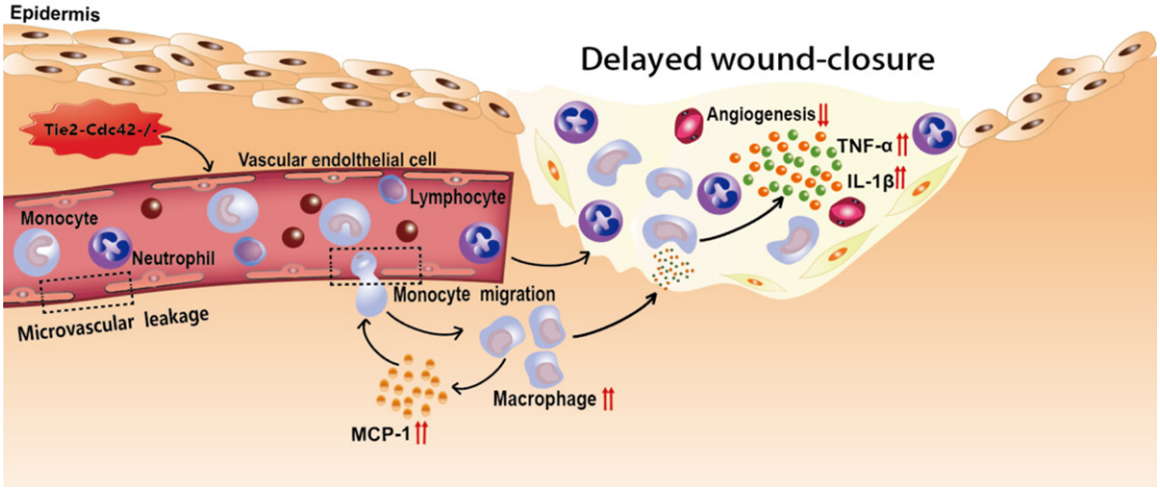

Figure 7. Schematic illustration of wound healing. A schematic illustration of skin wound healing when endothelial *Cdc42* is knocked out. In this study, we identified delayed wound healing in *Cdc42*$^{-/-}$ mice. Endothelial Cdc42 knockout resulted in decreased angiogenesis and increased macrophages and cytokine levels, which delayed reepithelialization.

Cdc42 knockout increased levels of MCP-1, IL-1β, and TNF-α

Next, we evaluated levels of cytokines because they are an important part of the healing process. The level of monocyte chemotactic protein 1 (MCP-1) was increased in wounds of *Cdc42*$^{-/-}$ mice compared with Ctrl mice (**Figure 6A**). The levels of the proinflammatory cytokines IL-1β and TNF-α were also increased in wounds of *Cdc42*$^{-/-}$ mice compared with Ctrl mice (**Figure 6B** and **6C**). These results suggest that *Cdc42* deletion induced excessive inflammation.

Discussion

In this study, using a mouse model of skin wound healing, we investigated the role of endothelial Cdc42 in regulating wound-healing processes, including inflammation, reepithelialization, and granulation tissue formation. To

our knowledge, this is the first time that endothelial Cdc42 deficiency has been shown to significantly impair wound healing. This wound-healing impairment was characterized by a delayed wound-closure rate, postponed reepithelialization, increased macrophage infiltration, increased cytokine levels, decreased angiogenesis, and irregular collagen deposition compared with wounds in Ctrl mice. These results suggest that endothelial Cdc42 plays a key role in neoangiogenesis and vascular permeability in wound-healing process.

Neoangiogenesis or vasculogenesis was initially thought to solely be embryogenesis, but in more recent years, vasculogenesis has been recognized as an essential process in adult vascular responses. For example, adults angiogenesis is a critical process in wound healing, and the formation of new blood vessels plays important roles in provisional granulation tissue formation [22]. In addition, the density of new blood vessels could determine wound-closure rate [23]. In our experiments, angiogenesis in the granulation tissue of *Cdc42*$^{-/-}$ mice was significantly reduced, which relates closely to the physiological role of Cdc42. Cdc42 binds GTP in the activated state and GDP in non-activated state, acting as a molecular switch for numerous cellular functions. Many studies have shown that Cdc42 plays roles in cell growth, proliferation, and migration. Olson et al. [24] inserted Cdc42 into Swiss3T3 fibroblasts through micro-injection and found that it accelerated the progression through the G1 phase and stimulated DNA synthesis. Lin et al. [25] transfected cells with a GTP-deficient mutant Cdc42, and the growth of cells was inhibited. Consistent with these observations, our results showed that Cdc42 deficiency in endothelial cells inhibited endothelial cells growth, proliferation, and migration, resulting in reduced angiogenesis in the wound.

Microvascular permeability is a key factor during wound-healing processes that is associated with local and/or systemic inflammatory response [26]. Our results showed that microvascular leakage was increased in the *Cdc42*$^{-/-}$ mouse model with full-thickness skin wounds. Additionally, more macrophages were found in the wounds of *Cdc42*$^{-/-}$ mice than Ctrl mice. As key inflammatory cells in wounds, macrophages contribute to the coordination of inflammation and angiogenesis during wound healing [27, 28]. While resident macrophages at the site of wound repair are present, the majority of macrophages are newly recruited from monocytes deployed to injured or reactive tissue [28]. MCP-1 is a chemokine that specifically recruits monocytes/macrophages. In our study, MCP-1 was higher in *Cdc42*$^{-/-}$ mice than in Ctrl mice. Although the mechanism underlying macrophage infiltration is not completely clear, it could be related to the role of Cdc42 in regulating endothelial cell permeability. Previous studies found that Cdc42 can enhance endothelial barrier function by inducing endothelial cell connections and interactions between a-catenin and the VE-cadherin complex [15]. Because T cells primarily accumulate during the tissue-remodeling phase [29], we observed no differences in numbers of T cells at the early stage of wound healing. Therefore, in our experiment, Cdc42-deficient endothelial cells decreased the formation of cell junctions, increased cell membrane permeability, and increased exudation of macrophages.

Wound healing is a complex process involving a variety of cells, including inflammatory cells, fibroblasts, keratinocytes, and endothelial cells, which produce numerous inflammatory cytokines such as IL-1β and TNF-α [30, 31]. In our study, the levels of IL-1β and TNF-α in *Cdc42*$^{-/-}$ mice were significantly higher than those in Ctrl mice. IL-1β and TNF-α have been shown to play dual roles in angiogenesis and vascular repair. On one hand, they are associated with increased numbers of macrophages in granulation tissue. Increased macrophage recruitment could lead to the release of more inflammatory cytokines that would further recruit and activate other inflammatory cells [32, 33]. On the other hand, increased cytokine levels reduce the number of blood vessels formed in granulation tissue, which could slow healing and result in a perpetual cycle [29].

We also observed that the wound healing in *Cdc42*$^{-/-}$ mice was significantly delayed to day 9 post-wounding from day 7 post-wounding in Ctrl mice based on complete closure of the skin wound. This result could be related to the decrease in neovascularization, which reduces the amount of nutrients in the wound bed, and/or the excessive inflammatory reaction and hyper-edema in and around the wound. While macrophages and increased vascular permeability can contribute to the regeneration of epi-

thelial cells to some degree [29, 34], excessive inflammatory responses can delay wound healing, as seen during infections [35, 36]. Reepithelialization is the resurfacing of a wound with new epithelium and involves both migration and proliferation of keratinocytes [37]. In this study, we found that *Cdc42*$^{-/-}$ mice had fewer keratinocytes in the proliferative phase in the wound tongue based on BrdU labeling, which could explain why wound closure was postponed in *Cdc42*$^{-/-}$ mice. The role of endothelial Cdc42 in skin wound healing is summarized in **Figure 7**.

In conclusion, in this study, we demonstrated that deletion of *Cdc42* in endothelial cells significant delayed wound closure. Our study suggests that Cdc42 is required for angiogenesis. The decreased angiogenesis and increased permeability lead to macrophage exudation, increased inflammatory cytokine production, and delayed reepithelialization and granulation formation, all of which could contribute to impaired wound closure.

Acknowledgements

We would like to thank Dr. Yi Zheng for providing the transgenic animals. This project was supported by the following grants: The National Natural Science Foundation of China (81402614, 81200060), the Natural Science Funding of Guangdong Province (2016A0303-10381, 2018A030313468), and Science and Technology Planning Project of Guangdong Province (2017A0202151888).

Disclosure of conflict of interest

None.

Address correspondence to: Dr. Yinghua Chen, Guangdong Provincial Key Laboratory of Construction and Detection in Tissue Engineering, Department of Histology and Embryology, School of Basic Medical Sciences, Southern Medical University, Guangzhou 510515, China. Tel: +86020-61648206; E-mail: mrchch@126.com; Dr. Guodong Hu, Department of Respiratory and Critical Care Medicine, Nanfang Hospital, Southern Medical University, Guangzhou 510515, China. E-mail: huguodong-123123@126.com

References

[1] Gurtner GC, Werner S, Barrandon Y and Longaker MT. Wound repair and regeneration. Nature 2008; 453: 314-321.

[2] Reinke JM and Sorg H. Wound repair and regeneration. Eur Surg Res 2012; 49: 35-43.

[3] Qi W, Yang C, Dai Z, Che D, Feng J, Mao Y, Cheng R, Wang Z, He X, Zhou T, Gu X, Yan L, Yang X, Ma JX and Gao G. High levels of pigment epithelium-derived factor in diabetes impair wound healing through suppression of Wnt signaling. Diabetes 2015; 64: 147-119.

[4] DiPietro LA. Angiogenesis and wound repair: when enough is enough. J Leukoc Biol 2016; 100: 979-984.

[5] Forsythe RO and Hinchliffe RJ. Assessment of foot perfusion in patients with a diabetic foot ulcer. Diabetes Metab Res Rev 2016; 32 Suppl 1: 232-238.

[6] Tanaka R, Vaynrub M, Masuda H, Ito R, Kobori M, Miyasaka M, Mizuno H, Warren SM and Asahara T. Quality-control culture system restores diabetic endothelial progenitor cell vasculogenesis and accelerates wound closure. Diabetes 2013; 62: 3207-3217.

[7] Wetzler C, Kämpfer H, Stallmeyer B, Pfeilschifter J and Frank S. Large and sustained induction of chemokines during impaired wound healing in the genetically diabetic mouse: prolonged persistence of neutrophils and macrophages during the late phase of repair. J Invest Dermatol 2000; 115: 245-253.

[8] Deng Y, Han X, Yao Z, Sun Y, Yu J, Cai J, Ren G, Jiang G and Han F. PPARalpha agonist stimulated angiogenesis by improving endothelial precursor cell function via a nlrp3 inflammasome pathway. Cell Physiol Biochem 2017; 42: 2255-2266.

[9] Reed BR and Clark RA. Cutaneous tissue repair: practical implications of current knowledge.II. J Am Acad Dermatol 1985; 13: 919-941.

[10] Schafer M and Werner S. Oxidative stress in normal and impaired wound repair. Pharmacol Res 2008; 58: 165-171.

[11] Etienne-Manneville S and Hall A. Rho GTPases in cell biology. Nature 2002; 420: 629-635.

[12] Vandenbroucke E, Mehta D, Minshall R and Malik AB. Regulation of endothelial junctional permeability. Ann N Y Acad Sci 2008; 1123: 134-145.

[13] Lv J, Zeng J, Zhao W, Cheng Y, Zhang L, Cai S, Hu G and Chen Y. Cdc42 regulates LPS-induced proliferation of primary pulmonary microvascular endothelial cells via ERK pathway. Microvasc Res 2017; 109: 45-53.

[14] Jin Y, Liu Y, Lin Q, Li J, Druso JE, Antonyak MA, Meininger CJ, Zhang SL, Dostal DE, Guan JL, Cerione RA and Peng X. Deletion of Cdc42 enhances ADAM17-mediated vascular endothelial growth factor receptor 2 shedding and impairs vascular endothelial cell survival and vasculogenesis. Mol Cell Biol 2013; 33: 4181-4197.

[15] Broman MT, Kouklis P, Gao X, Ramchandran R, Neamu RF, Minshall RD and Malik AB. Cdc42 regulates adherens junction stability and endothelial permeability by inducing alpha-catenin interaction with the vascular endothelial cadherin complex. Circ Res 2006; 98: 73-80.
[16] Hu GD, Chen YH, Zhang L, Tong WC, Cheng YX, Luo YL, Cai SX and Zhang L. The generation of the endothelial specific cdc42-deficient mice and effect of cdc42 deletion on the angiogenesis and embryonic development. Chin Med J (Engl) 2011; 124: 4155-4159.
[17] Godwin A, Sharma A, Yang WL, Wang Z, Nicastro J, Coppa GF and Wang P. Receptor-interacting protein kinase 3 deficiency delays cutaneous wound healing. PLoS One 2015; 10: e0140514.
[18] Cotsarelis G, Sun TT and Lavker RM. Label-retaining cells reside in the bulge area of pilosebaceous unit: implications for follicular stem cells, hair cycle, and skin carcinogenesis. Cell 1900; 61: 1329-1337.
[19] Bamberger C, Schärer A, Antsiferova M, Tychsen B, Pankow S, Müller M, Rülicke T, Paus R and Werner S. Activin controls skin morphogenesis and wound repair predominantly via stromal cells and in a concentration-dependent manner via keratinocytes. Am J Pathol 2005; 167: 733-47.
[20] Martinez-Ferrer M, Afshar-Sherif AR, Uwamariya C, de Crombrugghe B, Davidson JM and Bhowmick NA. Dermal transforming growth factor-beta responsiveness mediates wound contraction and epithelial closure. Am J Pathol 2010; 176: 98-107.
[21] Canesso MC, Vieira AT, Castro TB, Schirmer BG, Cisalpino D, Martins FS, Rachid MA, Nicoli JR, Teixeira MM and Barcelos LS. Skin wound healing is accelerated and scarless in the absence of commensal microbiota. J Immunol 2014; 193: 5171-5180.
[22] Li J, Zhang YP and Kirsner RS. Angiogenesis in wound repair: angiogenic growth factors and the extracellular matrix. Microsc Res Tech 2003; 60: 107-114.
[23] Eming SA, Brachvogel B, Odorisio T and Koch M. Regulation of angiogenesis: wound healing as a model. Prog Histochem Cytochem 2007; 42: 115-170.
[24] Olson MF, Ashworth A and Hall A. An essential role for Rho, Rac, and Cdc42 GTPases in cell cycle progression through G1. Science 1995; 269: 1270-1272.
[25] Lin A, Minden A, Martinetto H, Claret FX, Lange-Carter C, Mercurio F, Johnson GL and Karin M. Identification of a dual specificity kinase that activates the Jun kinases and p38-Mpk2. Science 1995; 268: 286-290.
[26] Yan M, Hu Y, Yao M, Bao S and Fang Y. GM-CSF ameliorates microvascular barrier integrity via pericyte-derived Ang-1 in wound healing. Wound Repair Regen 2017; 25: 933-943.
[27] Koh TJ and DiPietro LA. Inflammation and wound healing: the role of the macrophage. Expert Rev Mol Med 2011; 13: e23.
[28] Mahdavian Delavary B, van der Veer WM, van Egmond M, Niessen FB and Beelen RH. Macrophages in skin injury and repair. Immunobiology 2011; 216: 753-762.
[29] Eming SA, Krieg T and Davidson JM. Inflammation in wound repair: molecular and cellular mechanisms. J Invest Dermatol 2007; 127: 514-525.
[30] Werner S and Grose R. Regulation of wound healing by growth factors and cytokines. Physiol Rev 2003; 83: 835-870.
[31] Singer AJ and Clark RA. Cutaneous wound healing. N Engl J Med 1999; 341: 738-746.
[32] Lucas T, Waisman A, Ranjan R, Roes J, Krieg T, Muller W, Roers A and Eming SA. Differential roles of macrophages in diverse phases of skin repair. J Immunol 2010; 184: 3964-3977.
[33] Mirza R, DiPietro LA and Koh TJ. Selective and specific macrophage ablation is detrimental to wound healing in mice. Am J Pathol 2009; 175: 2454-2462.
[34] Rappolee DA, Mark D, Banda MJ and Werb Z. Wound macrophages express TGF alpha and other growth factors in vivo: analysis by mRNA phenotyping. Science 1988; 241: 708-712.
[35] Athanasopoulos AN, Economopoulou M, Orlova VV, Sobke A, Schneider D, Weber H, Augustin HG, Eming SA and Schubert U. The extracellular adherence protein (Eap) of Staphylococcus aureus inhibits wound healing by interfering with host defense and repair mechanisms. Blood 2006; 107: 2720-2727.
[36] Chavakis T, Hussain M, Kanse SM, Peters G, Bretzel RG, Flock JI, Herrmann M and Preissner KT. Staphylococcus aureus extracellular adherence protein serves as anti-inflammatory factor by inhibiting the recruitment of host leukocytes. Nat Med 2002; 8: 687-693.
[37] Yang L, Li W, Wang S, Wang L, Li Y, Yang X and Peng R. Smad4 disruption accelerates keratinocyte reepithelialization in murine cutaneous wound repair. Histochem Cell Biol 2012; 138: 573-582.

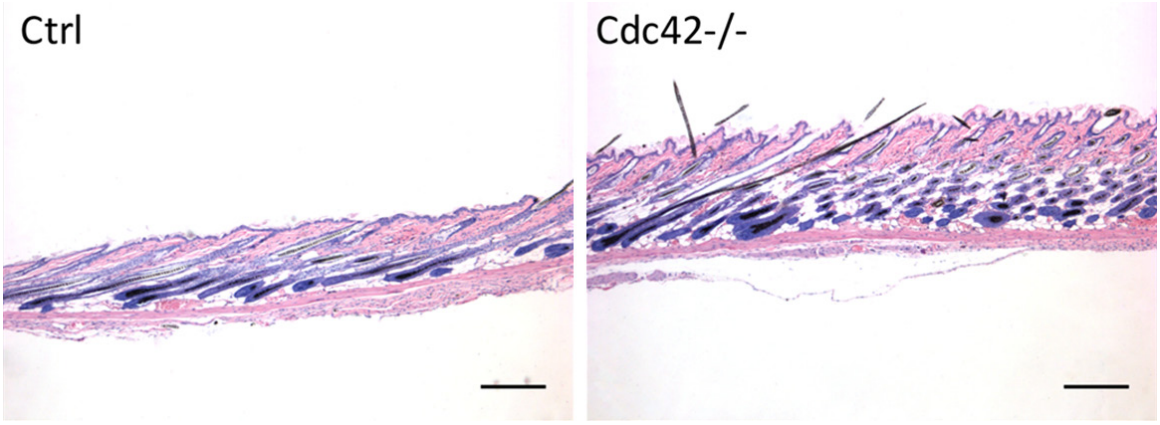

Supplementary Figure 1. No difference of histological sections of skin before wouding. Representative images of histological sections of skin from Ctrl and *Cdc42*$^{-/-}$ mice before wounding.